Environ. Sci. Technol. **2001**, *35,* 2949−2955

UV Photolysis of Nitrate: Effects of Natural Organic Matter and Dissolved Inorganic Carbon and Implications for UV Water Disinfection

CHARLES M. SHARPLESS AND KARL G. LINDEN*

Department of Civil and Environmental Engineering, Duke University, Box 90287, Durham, North Carolina 27708-0287

Nitrite (NO_2^-) formation during ultraviolet (UV) photolysis of nitrate was studied as a function of pH and natural organic matter (NOM) concentration to determine water-quality effects on quantum yields and overall formation potential during UV disinfection of drinking water with polychromatic, medium-pressure (MP) Hg lamps. Quantum yields measured at 228 nm are approximately 2 times higher than at 254 nm under all conditions studied. In the absence of NOM, NO_2^- quantum yields decrease with time. With addition of NOM, initial quantum yields increase, and the time-dependent decrease is eliminated. At 15 ppm dissolved organic carbon (DOC) as NOM, the quantum yield increases with time. Dissolved inorganic carbon significantly decreases NO_2^- yields at pH 8 but not pH 6, presumably by reaction of CO_2(aq) with peroxynitrite, a major intermediate in NO_2^- formation. The results indicate important and previously unrecognized roles for NOM and CO_2(aq) in nitrate photolysis. When photolysis was carried out using the full spectrum MPUV lamp and germicidally relevant UV doses, NO_2^- concentrations remained well below the U.S. maximum contaminant level of 1 ppm N, even with nitrate initially present at 10 ppm N. Under current U.S. regulations, NO_2^- formation should not pose a significant problem for water utilities during UV disinfection of drinking water with MP Hg lamps.

Introduction

Ultraviolet light (UV) is a proven technology for disinfecting wastewater and is currently being considered for use as a primary disinfectant for drinking water. Recent work has demonstrated its effectiveness against many human pathogens, including *Cryptosporidium* and *Giardia*, which are resistant to traditional disinfection techniques (*1, 2*). The use of UV for drinking water disinfection can reduce the necessary chlorine dose, leading to lower concentrations of disinfection byproducts (DBPs). For these reasons, UV is under consideration as an acceptable technology to meet upcoming regulations under the proposed Stage 2 DBP Rule and the Long-Term 2 Enhanced Surface Water Treatment Rule. UV is widely used for drinking water disinfection in Europe, where over 2000 installations exist. Of the currently available UV technologies, the most well-known and frequently used are low- and medium-pressure Hg arc lamps (LPUV and MPUV, respectively). The former produces essentially monochromatic light at 254 nm, while the latter produces polychromatic light over a wide range of UV and visible wavelengths.

One concern that surrounds the use of UV for water treatment is whether nitrite (NO_2^-) formed from nitrate (NO_3^-) photolysis will pose a health threat. When LPUV is used for disinfection purposes, there appears to be little reason for concern. Research has shown that even with NO_3^- at the maximum allowable contaminant level (MCL) of 10 ppm N, NO_2^- formation is negligible at UV doses relevant to disinfection (up to 250 mJ/cm^2) (*3*). While higher NO_3^- levels, such as are sometimes present in wastewater, and/or higher UV doses (e.g., for chemical oxidation) may produce unacceptable amounts of NO_2^-, the upper limits for these parameters have not been rigorously defined.

With regard to NO_2^- formation during UV disinfection, LPUV should be quite safe. The potential for NO_2^- formation during disinfection with polychromatic MPUV sources is greater, but whether there are serious associated health risks and what effect(s) water quality may have has not been fully established. It is known that the quantum yield for NO_2^- formation is higher at shorter wavelengths (*4*), such as are present with MPUV, but no published studies have addressed the relevance of this phenomenon to water disinfection scenarios. German water treatment systems using MPUV are required to incorporate specially doped quartz sleeves, which cut off wavelengths below 240 nm (*5*) and concomitantly reduce the germicidal efficiency of the lamps. Such a practice finds no justification in the research literature, although it increases the cost of MPUV implementation by reducing the germicidal UV output. In fact, recent work on MPUV using typical nondoped quartz sleeves and raw source water (NO_3^- levels of 4.6 ppm) found that even with UV doses as high as 1000 mJ/cm^2 (approximately 10 times the likely UV disinfection dose for drinking water) NO_2^- did not exceed the German regulatory limit of 0.1 ppm (*6*).

Although this seems to indicate that MPUV water treatment should not produce excessive NO_2^- concentrations, the study did not address water matrix effects. One natural water constituent that is likely to influence the extent of NO_2^- formation is dissolved organic matter. It is known that organic compounds can increase NO_2^- quantum yields, presumably by competing with NO_2^- for $^\bullet$OH radical (*4, 7*). However, previous researchers have often used dissolved organic carbon (DOC) levels that are orders of magnitude higher than in drinking water sources. Furthermore, all of the compounds investigated to date have been simple, uncolored, and of low molecular weight: no research exists that addresses the effects of natural organic matter (NOM), such as humic and fulvic acids. Another water constituent that may be important is dissolved inorganic carbon. Aside from NOM, CO_3^{2-} and HCO_3^- are two of the most significant natural $^\bullet$OH radical scavengers (*8, 9*) and may thus increase NO_2^- yields. However, recent biochemical research has definitively proven that dissolved CO_2 reacts with peroxynitrite (*10, 11*), which is a crucial precursor of NO_2^- in NO_3^- photolysis (*12*−*14*); in the absence of reducing agents, the net effect of this reaction is to catalyze the isomerization of peroxynitrite into NO_3^-. Thus, it is of interest to determine the effect of dissolved inorganic carbon on NO_3^- photolysis in natural waters.

This research has addressed the effects of pH, wavelength, NOM, and dissolved inorganic carbon on NO_2^- formation. The results show that the mechanism of NO_2^- formation via

* Corresponding author phone: (919)660-5196; fax: (919)660-5219; e-mail: kglinden@duke.edu.

10.1021/es002043l CCC: $20.00
Published on Web 06/07/2001

NO_3^- photolysis is highly dependent on these parameters. They also demonstrate a significant role for dissolved inorganic carbon that has been previously overlooked as well as effects of NOM that appear quite distinct from those of uncolored, low molecular weight organic compounds. These findings have implications for UV disinfection operating parameters, and more fundamentally, they suggest new reaction pathways that should be considered in the mechanism of NO_3^- photolysis in natural waters.

Experimental Materials and Methods

Reagents. All chemicals used in this research were analytical grade and were used as received. Dilute solutions (0.1 or 0.01 M) of NaOH and HCl (both Mallinckrodt) were used to adjust pH. All solutions were prepared using deionized (DI) water. Suwannee River natural organic matter (NOM) was obtained from the International Humic Substances Society (IHSS) and used as received. This NOM was isolated by reverse osmosis, treated with cation exchange to remove complexed metals, and freeze-dried; more details about the procedure can be obtained from IHSS. Glassware cleaning always included a nitric acid soak followed by thorough rinsing with DI water to remove any trace metal impurities that could catalyze the decomposition of peroxynitrite to NO_2^- (*13*).

Experimental Overview. Two sets of experiments were conducted: measuring NO_2^- quantum yields as a function of wavelength and water quality and measuring NO_2^- concentrations under typical MPUV disinfection conditions. All experiments were performed at pH 6 and pH 8, but the initial NO_3^- concentrations were different in the two sets of experiments. For quantum yield experiments, it was 0.098 M, while for disinfection-type experiments it was 0.714 mM (10 ppm as N). In most experiments, 1 mM $NaHCO_3$ was included, and instances where it was not are discussed in detail below. Finally, the effect of NOM was studied in both quantum yield and disinfection-type experiments at DOC levels of 0, 5, and 15 ppm.

Experimental Solutions. A stock solution of NOM was prepared in the following manner. Approximately 50 mg of NOM was weighed into a 50-mL beaker, a stirbar was added, and the beaker was filled to about the 30-mL mark with DI water. Dilute NaOH was added dropwise while stirring until the pH was approximately 9. The solution was stirred for 2−3 h, at which point it was filtered (0.45 μm) and then stored for future use (4 °C); stock solutions were kept no longer than 3 weeks. DOC measurements were performed in triplicate using a Tekmar-Dohrmann (Cincinnati, OH) Apollo 9000 carbon analyzer, and NOM stock solutions contained approximately 450 ppm DOC.

Nitrate solutions without DOC were made by dissolving an appropriate amount of solid KNO_3 in freshly prepared 1 mM $NaHCO_3$ and diluting with 1 mM $NaHCO_3$ as necessary. Nitrate solutions containing DOC (as NOM) were prepared by diluting the NOM stock to the appropriate concentration in KNO_3 solutions prepared as just described. The pH was then adjusted to the desired value, and the solution was left covered overnight at room temperature. The following morning, fine adjustments to the pH were made, and the solutions were then used immediately in photolysis experiments. Due to CO_2 exchange during the overnight equilibration, the dissolved inorganic carbon (DIC) concentrations differed between the solutions at pH 6 and pH 8. Determinations of DIC were made on samples immediately after photolysis. Regardless of DOC content, samples at pH 8 showed no change from the initial level of 12 ppm DIC (1 mM). The samples at pH 6, however, had DIC values ranging from roughly 2 to 6 ppm. Interestingly, this variability has little effect, as demonstrated by the results of experiments without $NaHCO_3$ (see below).

NO_2^- Analysis. Colorimetry was used for NO_2^- analysis. The absorbance was measured on a Cary 100-Bio spectrophotometer (1 cm path length), and the procedure was essentially that given in Standard Methods, Method 4500, NO_2^- (*16*), with modifications to the volumes of sample and reagents employed. Calibration curves were constructed using fresh $NaNO_2$ in water matrices identical to those used for photolysis experiments. These curves were linear from the highest concentration measured (approximately 7 μM) down to the detection limit (defined as the blank signal plus 3σ), which was 70 nM with 0 ppm DOC and 84 nM with 15 ppm DOC. The quantification limits (blank plus 6σ) were 140 and 168 nM, respectively. Interestingly, NOM not only increased the blank baseline but also decreased the analytical response (i.e., the calibration slope decreased as DOC levels increased). For a given water matrix, the calibration slopes were identical at pH 6 and pH 8 within the standard deviations of triplicates.

Photolysis Experiments. Photolysis experiments were performed with a 1 kW MP Hg lamp (Hanovia Co., Union, NJ) housed in a bench-scale UV irradiation device (Calgon Carbon Co., Pittsburgh, PA). Experiments were conducted with either the full lamp output (unfiltered) or with bandpass filters (∼10 nm bandwidth, Andover Co., Salem, NH) placed in the light path. In both cases the incident irradiance was determined by ferrioxalate actinometry (*17*) using an experimental geometry identical to that for the photolysis experiments. The incident irradiance was calculated from the Fe^{2+} production rate using a value of 1.25 for the quantum yield below 300 nm, as reported by Murov (*17*). For unfiltered experiments, the incident irradiance in the 200−300-nm range was determined from the difference between Fe^{2+} production rates with and without a 1/4-in.-thick Pyrex plate in the light path. Pyrex of this thickness actually cuts off some light between 300 and 320 nm, so the irradiance determined in this fashion is slightly overestimated. Daily corrections for lamp intensity fluctuations were made by monitoring the irradiance with a calibrated radiometer (International Light model 1700) and comparing the reading to that obtained during actinometry measurements.

In a typical photolysis experiment, a 20-mL sample was irradiated with gentle stirring in a 50 × 35 mm crystallization dish (16.6 cm^2 surface area) for periods of 15 or 17 min (filtered and unfiltered experiments, respectively). For samples at pH 6, the pH increased to anywhere from 6.5 to 7.0 during the experiment due to CO_2 exchange. This should have little effect since there is virtually no difference in the NO_2^- quantum yield over the pH 6−7 range (*7*, *18*). To verify this, some experiments were performed with the addition of a 1 mM phosphate buffer; no difference was observed with the pH held constant.

At evenly spaced time intervals, a 0.75-mL sample was removed for NO_2^- analysis. This caused a decrease in solution depth as samples were taken, which increases the NO_2^- production rate over time. The data presentation accounts for the depth decrease by plotting NO_2^- concentrations and quantum yields versus light absorbed by NO_3^-. In the case of irradiation with the unfiltered lamp, NO_2^- concentrations are presented as a function of average UV dose, which was calculated with the depth decrease accounted for.

Quantum Yield Determinations. The reported NO_2^- quantum yields are integral quantum yields at a given time, t, designated $\Phi_{NO_2^-}(t)$. This is defined as

$$\Phi_{NO_2^-}(t) = \frac{n_{NO_2^-}(t)}{Es_{a,NO_3^-}(t)} \quad (1)$$

where $n_{NO_2^-}(t)$ represents the moles of NO_2^- measured at time t, and $Es_{a,NO_3^-}(t)$ is einsteins absorbed by NO_3^- at time

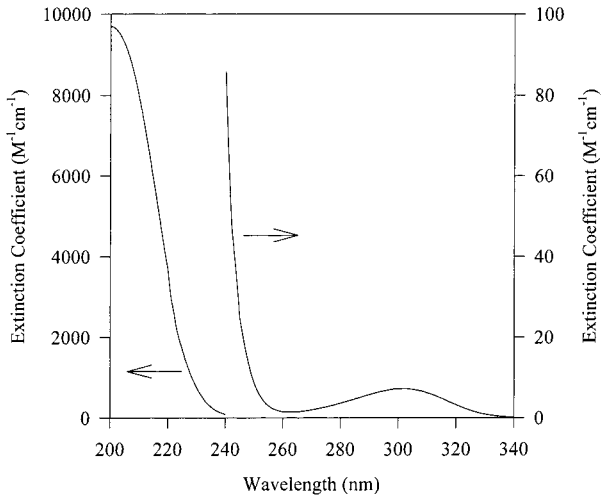

FIGURE 1. Molar absorbance spectrum of NO_3^-.

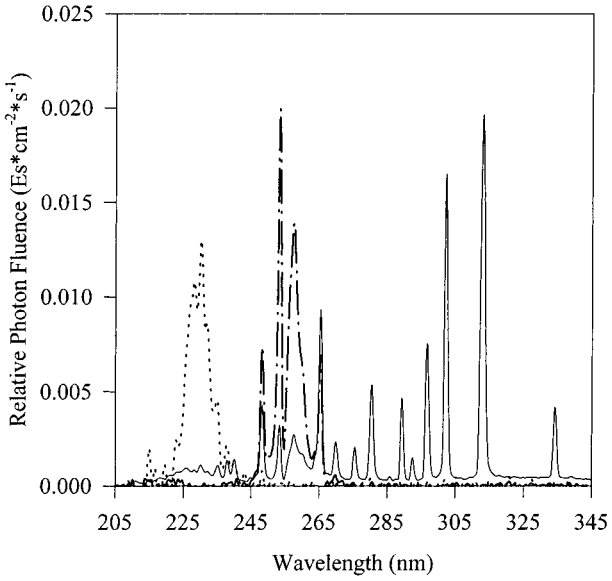

FIGURE 2. Normalized emission spectra of the MP lamp: unfiltered (solid line) and with 254-nm (long dashes) and 228-nm (short dashes) band-pass filters.

t (summed over all wavelengths). The time dependence is given explicitly here because $\Phi_{NO_2^-}$ varies with the amount of absorbed light, as demonstrated by other researchers (*7*, *18*, *19*). It is important to note that these values are overall quantum yields for NO_2^- formation via all possible reaction pathways. Thus, NO_2^- formed from peroxynitrite ($ONOO^-$) decomposition (*13*, *14*) is included in the measurements. In the context of the present work, this is appropriate since we are interested simply in the amount of NO_2^- produced during aqueous-phase photolysis.

The quantity $Es_{a,NO_3^-}(t)$ was determined from the average solution irradiance corrected for light screening by NOM (*8*), the known concentration of NO_3^-, its absorbance spectrum (Figure 1), and the output spectrum of the lamp, which was measured with a fiber optic spectrometer (model S2000, Ocean Optics, Inc., Dunedin, FL) and normalized (Figure 2).

As mentioned previously, it is known that the quantum yield of NO_2^- formation is higher at shorter wavelengths (*4*). Because a polychromatic light source was used in these experiments, the quantum yields reported here are wavelength averaged. Making the time dependence of $\Phi_{NO_2^-}$ implicit and the wavelength dependence explicit, this can be expressed as

$$\Phi_{NO_2^-} = \frac{\sum_\lambda Es_{a,NO_3^-}(\lambda)\Phi_{NO_2^-}(\lambda)}{\sum_\lambda Es_{a,NO_3^-}(\lambda)} \quad (2)$$

where the symbol λ in parentheses indicates the wavelength dependence of both the light absorption and the quantum yield.

Results and Discussion

Effect of Wavelength, pH, and Dissolved Inorganic Carbon on $\Phi_{NO_2^-}(t)$. Figure 3 shows NO_2^- concentrations as a function of Es_{a,NO_3^-} for both pH values and wavelengths investigated. Figure 4 shows these results plotted in terms of $\Phi_{NO_2^-}$. In these experiments, the total irradiation time was 15 min. In this and the following data, some replicates were performed several weeks apart, during which time the lamp output varied. Thus, the total energy delivered in those experiments varied somewhat between replicates, which is shown by the inclusion of error bars for the *x*-axis.

At 254 nm, the initial quantum yield increases only slightly in going from pH 6 to pH 8, and the absolute values compare well to previous reports under similar conditions (*7*). A number of researchers have noted a similar pH dependence of $\Phi_{NO_2^-}$ (*7*, *18*–*21*), and this is discussed in more detail below. Another important feature of the 254-nm data is the decrease in $\Phi_{NO_2^-}$ at both pH 6 and pH 8 as Es_{a,NO_3^-} increases, and other studies have demonstrated that NO_2^- somehow serves as an inhibitor of its own production (*4*). While this is always observed at neutral and acidic pH, there are conflicting reports about whether it occurs in basic solution (*7*, *18*, *19*). The discrepancies may be due to differences in Es_{a,NO_3^-}, but it is difficult to tell because these values are often not reported and are sometimes impossible to estimate from the given information. As illustrated in the figures, a downward curvature in the plots of NO_2^- versus Es_{a,NO_3^-} was consistently observed at pH 8 in these experiments.

With photolysis at 228 nm, the quantum yields are higher at pH 8 than at pH 6. These yields cannot be compared to literature values since comparable data have not been published for these combinations of wavelength and pH. However, quantum yields of approximately 0.25 at similar wavelengths have been reported for pH 11.5 (*20*, *21*), and our lower values are expected given the lower pH. One study did concern NO_3^- photolysis at identical wavelength and pH values but did not report quantum yields (*19*). However, NO_2^- concentrations were given and were higher at pH 8 than at pH 6, similar to our observations.

The accepted explanation for the pH dependence of $\Phi_{NO_2^-}$ is the influence of the acid–base pair ONOOH/$ONOO^-$, for which $pK_a = 6.8$ (*22*). How these species are formed during NO_3^- photolysis is still a matter of debate, but the preponderance of evidence indicates that they do form when photolysis is carried out below 280 nm (*4*, *12*–*14*). Two previously proposed mechanisms are the isomerization of excited-state NO_3^- (reaction 3) and cage recombination of $^\bullet OH$ and $^\bullet NO_2$ radicals produced from excited-state NO_3^- (reaction 4) (*4*):

$$NO_3^{-*} \rightarrow ONOO^- \quad (3)$$

$$NO_3^{-*} \rightarrow [^\bullet NO_2 + {}^\bullet O^-] + H^+ \rightarrow {}^\bullet NO_2 + {}^\bullet OH \rightarrow ONOOH \quad (4)$$

$$ONOOH \rightarrow ONOO^- + H^+ \quad pK_a = 6.8 \quad (5)$$

Peroxynitrous acid undergoes rapid rearrangement to nitric acid followed by dissociation to produce NO_3^- via reaction

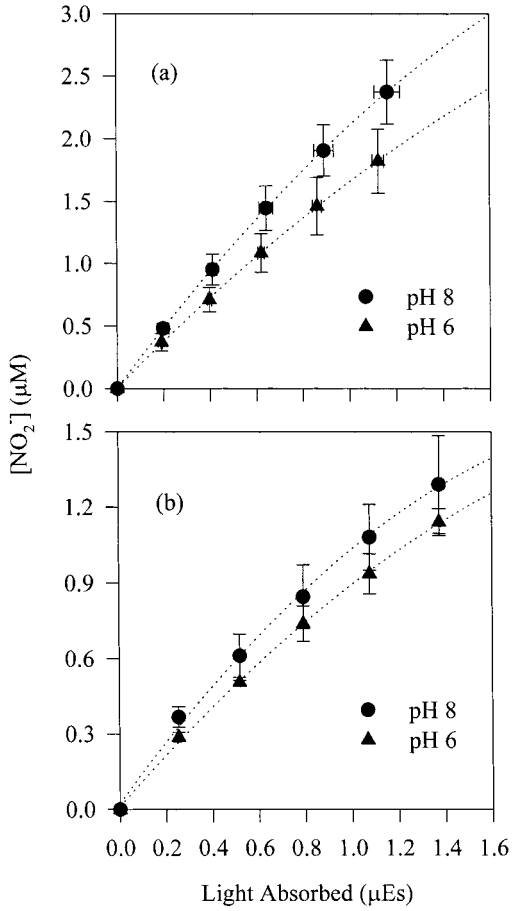

FIGURE 3. Nitrite concentrations as a function of Es absorbed with 0 ppm DOC: (a) 228 nm, (b) 254 nm.

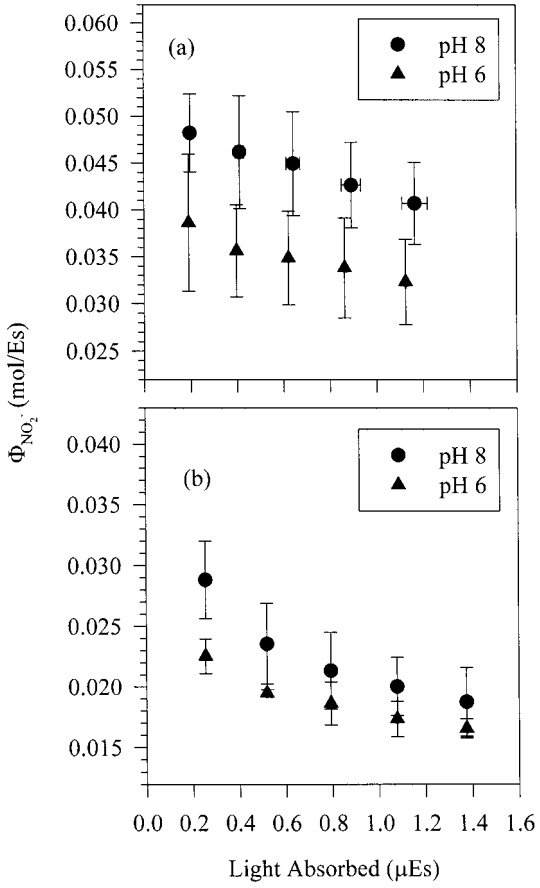

FIGURE 4. Nitrite quantum yields as a function of Es absorbed with 0 ppm DOC: (a) 228 nm, (b) 254 nm.

6 (*4*, *12*, *23*−*26*). On the other hand, the relatively stable peroxynitrite ($ONOO^-$) can decompose to produce NO_2^- through a complex mechanism with the overall stoichiometry given in reaction 7. The notation X is used here to stand for various intermediates because a proper discussion of the mechanism would be lengthy and is inappropriate here. However, there are some important points worth noting in the present context. First, there are several radical reactions involved, many of which involve the species $^{\bullet}NO_2$, $^{\bullet}OH$, $^{\bullet}O_2^-$, or $^{\bullet}NO$ (*25*). Second, protonation of $ONOO^-$ or its interaction with other Lewis acids (e.g., CO_2) leads to rapid formation of NO_3^- via reactions analogous to reaction 6 that proceed through steps involving fairly strong oxidants (*25*) Third, the effects of organic $^{\bullet}OH$ scavengers on this reaction are quite complex and are presently very poorly understood (*25*). Finally, in the specific case of NO_3^- photolysis, photolytic decomposition of $ONOO^-$ may perhaps be relevant (*4*, *7*, *12*, *19*), although its significance is difficult to assess in our experiments in the absence of $ONOO^-$ concentration data and the lack of published quantum yields for the reaction.

$$ONOOH \rightarrow [^{\bullet}NO_2 + {}^{\bullet}OH] \rightarrow HNO_3 \rightarrow NO_3^- + H^+ \quad (6)$$

$$ONOO^- \rightarrow X \rightarrow NO_2^- + \frac{1}{2}O_2\ (X = \text{intermediates}) \quad (7)$$

In basic solutions, therefore, $ONOO^-$ should accumulate and increase $\Phi_{NO_2^-}$ by reaction 7. Another way that $ONOO^-$ may increase $\Phi_{NO_2^-}$ is by acting as an $^{\bullet}OH$ scavenger (reaction 8, $k = 5 \times 10^9\ M^{-1}\ s^{-1}$), thus protecting NO_2^- from reaction with $^{\bullet}OH$ ($k = 1 \times 10^{10}\ M^{-1}\ s^{-1}$) (*4*):

$$ONOO^- + {}^{\bullet}OH \rightarrow {}^{\bullet}NO + O_2 + OH^- \quad (8)$$

A conspicuous difference between the experimental conditions used here and those of previous studies is the presence of significant amounts of DIC. Recent investigations into the biochemical role of $ONOO^-$ (produced in vivo by reaction between $^{\bullet}NO$ and $^{\bullet}O_2^-$) have shown that it reacts quickly with CO_2(aq) to form the adduct $ONOOCO_2^-$ ($k = 3 \times 10^4\ M^{-1}\ s^{-1}$) (*10*, *27*). In the absence of reducing agents, the adduct rearranges through an as yet unknown mechanism to yield NO_3^- and CO_2 (i.e., CO_2 is a catalyst for $ONOO^-$ isomerization to NO_3^-) (*28*, *29*). Thus, during NO_3^- photolysis CO_2 should lower the yield of NO_2^-. However, only two reports have been published involving the use of the buffer HCO_3^-/CO_3^{2-} at pH 10.3, and they are contradictory. Daniels et al. mentioned observing a decreased rate with this buffer but did not give further details (*18*). In contrast, Shuali et al. reported that there was no effect of the carbonate buffer (*19*).

To clarify the role of DIC, experiments were performed at 228 nm without the addition of $NaHCO_3$. This wavelength was chosen because NO_2^- yields are higher than at 254 nm and differences are thus more likely to be detected. Figure 5 illustrates the data obtained with and without $NaHCO_3$. Phosphate buffer was used in some experiments (included in the data shown) but had no effect on the results at either pH. Clearly, DIC lowers the NO_2^- yields at pH 8. At pH 6, however, there is essentially no effect. This pH dependence is easily understood by considering that it is $ONOO^-$ ($pK_b = 7.2$) and not ONOOH that reacts with CO_2.

The relative importance of the reaction pathway involving CO_2 in these experiments can be quantified. To do so, we

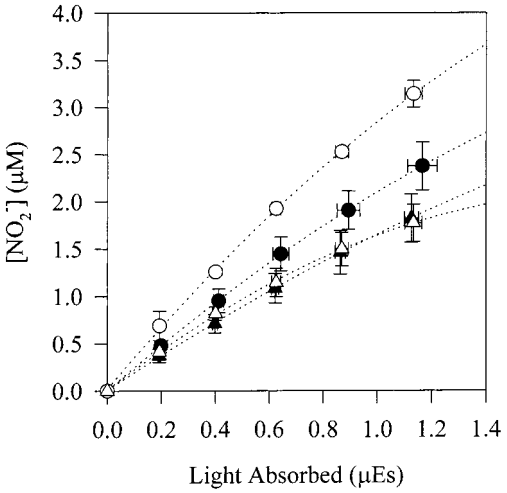

FIGURE 5. Nitrite concentrations as a function of Es absorbed at 228 nm with 0 ppm DOC: effect of $NaHCO_3$. Open symbols, no $NaHCO_3$; filled symbols, 1 mM $NaHCO_3$ initially; circles, pH 8; triangles, pH 6.

first calculate the pseudo-first-order rate constant, k', for reaction 9 assuming that CO_2, determined from the measured pH and final DIC values, is in excess over $ONOO^-$ and using the pH independent second-order rate constant $k = 3 \times 10^4$ M^{-1} s^{-1} (*10*):

$$ONOO^- + CO_2 \rightarrow ONOOCO_2^- \qquad (9)$$

Under the conditions used here, k' ranges from 2 to 6 s^{-1} at pH 6 and is equal to 0.6 s^{-1} at pH 8 (the variability at pH 6 is due to the DIC variability noted in the Experimental Section). For simplicity, the primary competing reaction is assumed to be the decay of $ONOO^-$ via reaction 10, but it is noted that the situation is likely more complicated than this (*25, 30*):

$$ONOO^- \rightarrow NO_3^- \qquad (10)$$

The apparent first-order rate constant for this reaction can be estimated from the expression (*12, 28*)

$$k'' = \frac{k_0[H^+]}{[H^+] + K_a} \qquad (11)$$

where k'' is the pH-dependent rate constant, K_a is the acid dissociation constant, and k_0 is the pH-independent rate constant for isomerization of ONOOH to HNO_3, approximately 1.3 s^{-1} (*4*). This calculation gives k'' values of 1 and 0.08 s^{-1} at pH 6 and pH 8, respectively. These compare well with recently measured values of 0.61 and 0.08 s^{-1} (*26*) and of 0.76 and 0.046 s^{-1} (*29*). Given these rate constants, the reaction of $ONOO^-$ with CO_2 should proceed roughly 2−6 and 10 times faster than the first-order decay process at pH 6 and pH 8, respectively. The catalytic contribution of CO_2 to NO_3^- formation from $ONOO^-$ is therefore highly significant and is large enough at pH 8 to be easily detected in these experiments. Dissolved CO_2 is clearly an important feature of NO_3^- photolysis in natural waters that has been previously overlooked.

Influence of NOM on $\Phi_{NO_2^-}$. The effect of NOM on $\Phi_{NO_2^-}$ is illustrated in Figures 6 and 7. The addition of either 5 or 15 ppm DOC as Suwannee River NOM increases $\Phi_{NO_2^-}$ relative to its value in the 0 ppm DOC system. Control experiments

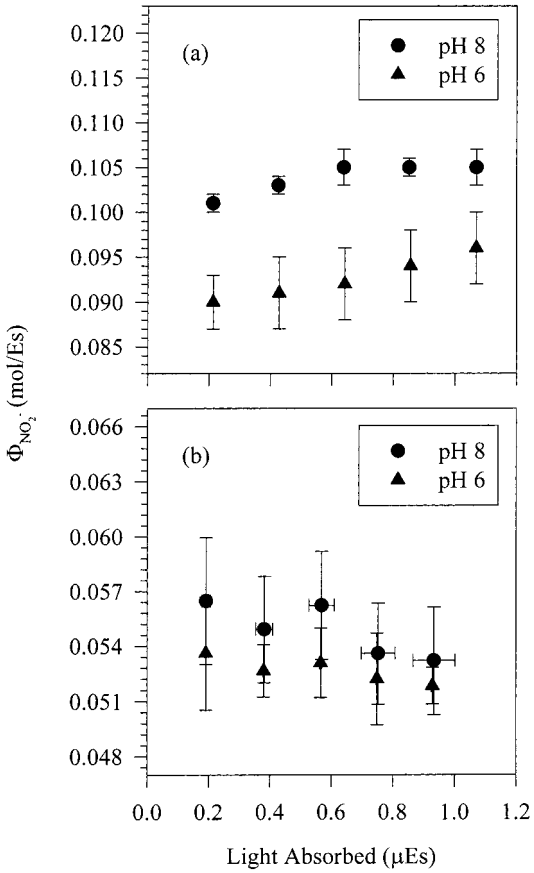

FIGURE 6. Nitrite quantum yields as a function of Es absorbed with 5 ppm DOC: (a) 228 nm, (b) 254 nm.

indicated that NOM did not produce NO_2^- by dark reaction with NO_3^-, nor was NO_2^- production observed by irradiating NOM in the absence of NO_3^-. For these experiments, it was desired to measure $\Phi_{NO_2^-}$ in water that simulated natural DOC and DIC conditions. Therefore, $NaHCO_3$ was present in all the solutions.

The dependence of $\Phi_{NO_2^-}$ on Es_{a,NO_3^-} in the presence of NOM is distinctly different from that in the 0 ppm DOC solutions. At 5 ppm DOC, photolysis leads to a virtually constant NO_2^- production rate (constant $\Phi_{NO_2^-}$). With photolysis at 254 nm, there is a slight trend toward decreasing $\Phi_{NO_2^-}$ with Es_{a,NO_3^-}, while at 228 nm there is a slight trend toward increasing $\Phi_{NO_2^-}$ with Es_{a,NO_3^-}. Also, at 254 nm, the values of $\Phi_{NO_2^-}$ at pH 8 are marginally higher than at pH 6, similar to the 0 ppm DOC solutions. At 228 nm, $\Phi_{NO_2^-}$ is clearly higher at pH 8 than at pH 6. When 15 ppm DOC is added, $\Phi_{NO_2^-}$ actually increases with Es_{a,NO_3^-} at both wavelengths and pH values, and at both wavelengths $\Phi_{NO_2^-}$ is clearly higher at pH 8. It is also noteworthy that in 15 ppm DOC, $\Phi_{NO_2^-}$ does not level off within the time frame of these experiments. Thus, the addition of NOM not only increases the magnitude of $\Phi_{NO_2^-}$ but also counteracts the decrease in $\Phi_{NO_2^-}$ with Es_{a,NO_3^-} that is observed in the 0 ppm DOC solutions, at first leading to a linear NO_2^- production rate (5 ppm DOC) and then an increasing NO_2^- production rate (15 ppm DOC). Apparently, this phenomenon has not previously been reported.

The addition of organic compounds to solutions at pH < 9 has been reported by several other researchers to increase $\Phi_{NO_2^-}$ (*7, 18, 21*). The principal explanation for this effect is that organic compounds scavenge $^{\bullet}OH$, which prevents its reaction with NO_2^- and with $^{\bullet}NO_2$, the latter being a potentially important intermediate via any of the

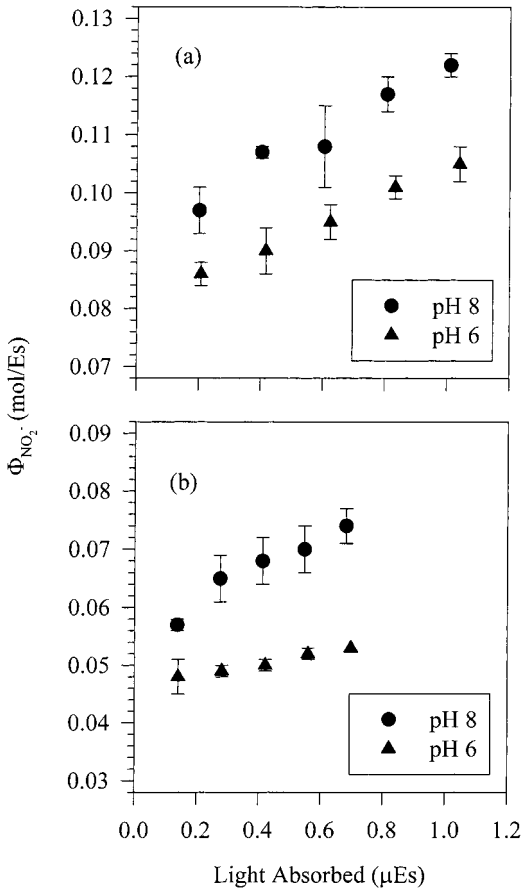

FIGURE 7. Nitrite quantum yields as a function of Es absorbed with 15 ppm DOC: (a) 228 nm, (b) 254 nm.

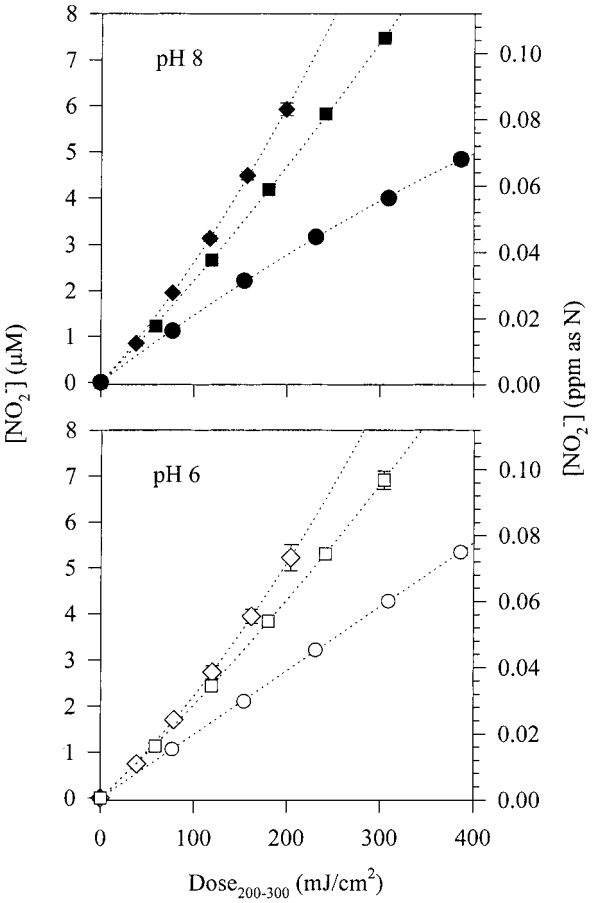

FIGURE 8. Nitrite concentrations as a function of average UV dose (mJ/cm^2 in the 200−300-nm range) during NO_3^- photolysis with the unfiltered MP lamp at pH 6 and pH 8. DOC concentrations: 0 (circles), 5 (squares), and 15 ppm (diamonds).

following reactions (*4*):

$$2^{\bullet}NO_2 \rightarrow N_2O_4 + H_2O \rightarrow NO_2^- + NO_3^- + 2H^+ \quad (12)$$

$$^{\bullet}NO_2 + {}^{\bullet}NO \rightarrow N_2O_3 + H_2O \rightarrow 2NO_2^- + 2H^+ \quad (13)$$

$$^{\bullet}NO_2 + {}^{\bullet}O_2^- \rightarrow NO_2^- + O_2 \quad (14)$$

Here, NO$^{\bullet}$ may be produced via reaction 8, among other possibilities. Inorganic $^{\bullet}$OH scavengers should lead to equivalent results (except in the case of HCO_3^-/CO_3^{2-}, when CO_2 is present), and this has been demonstrated to some extent for Br^- and As^{3+} (*18*, *21*). Although reactions 12 and 13 imply that pH decreases with time, preceding reactions produce equivalent amounts of OH^-. In reaction 13, $^{\bullet}O^{2-}$ may be produced as an intermediate in reaction 7 or, in the specific case of organic $^{\bullet}$OH scavengers, from secondary reactions of organic radicals (*7*). Similar to previous reports, a DOC-dependent increase in the initial $\Phi_{NO_2^-}$ values was observed. However, the increase in $\Phi_{NO_2^-}$ with Es_{a,NO_3^-} reported here appears to have never previously been observed. The reason(s) for this increase are currently unknown but may relate to either light screening by NOM (protecting some unknown intermediate from photolysis), reactions of NOM with $ONOOCO_2^-$, or both. Further experiments are currently planned to investigate these possibilities.

With regard to how NOM may influence the CO_2-dependent reactions, a brief discussion is in order. For a few years now, biochemists have recognized that CO_2 catalyzes $OONO^-$-initiated oxidations (*11*, *27*, *31*). These reactions clearly proceed through the $ONOOCO_2^-$ intermediate, and recent research has shown that approximately 35% of this species decays according to the reaction (*28*, *29*):

$$ONOOCO_2^- \rightarrow {}^{\bullet}CO_3^- + {}^{\bullet}NO_2 \quad (15)$$

Both of these radicals are capable of oxidizing many natural organic compounds (E_0, $^{\bullet}CO_3^-/CO_3^{2-} = 1.5$ V; E_0, $^{\bullet}NO_2/NO_2^- = 1.04$ V) (*23*, *28*). Therefore, in natural waters containing both CO_2 and DOC, organic compounds may increase NO_2^- yields by either (a) reacting with $^{\bullet}CO_3^-$, allowing $^{\bullet}NO_2$ to participate in reactions 12−14 or (b) reducing $^{\bullet}NO_2$ to form NO_2^- directly. This set of reactions, in addition to $^{\bullet}$OH scavenging, may be important in explaining how DOC increases $\Phi_{NO_2^-}$ in natural waters.

NO_2^- Production with the Unfiltered MP Hg Lamp. The results of NO_3^- photolysis with the unfiltered MP lamp are shown in Figure 8. In these experiments, the concentration of NO_3^- was set at the MCL of 10 ppm as N (7.14×10^{-4} M) as specified in the Safe Drinking Water Act. The *x*-axis in the figure is the *average* UV dose (as opposed to incident dose) over the 200−300-nm range in mJ/cm^2, which is calculated using the absorbance of the water sample, including that from NO_3^-. The use of these units is consistent with UV disinfection literature except that the germicidal UV dose is roughly 60% of the total dose in the 200−300-nm range. The solutions were irradiated for a fixed time of 17 min, and because of light screening by NOM, the average dose decreases with increasing DOC. Thus, in the absence of NOM, the final dose delivered is approximately 400 mJ/cm^2, while for 15 ppm DOC it is around 200 mJ/cm^2. Even at the low end, these doses are typically 2−4× higher than those required for water disinfection (*2*).

The NO_2^- quantum yields corresponding to the data in Figure 8 are similar to those observed with irradiation at 228 nm. This shows that the shorter wavelengths dominate the NO_3^- photolysis behavior as should be expected from the NO_3^- absorbance spectrum. From the curvature in the plots, it is clear that NOM has the same effect as observed in the quantum yield experiments. The DOC-dependent increase in $\Phi_{NO_2^-}$ is also evident by comparing the NO_2^- concentrations at 200 mJ/cm^2. Although it is not proven explicitly here, there is good reason to believe that the similarity of the NO_2^- concentrations at both pH 6 and pH 8 in these samples reflects the influence that DIC has on lowering $\Phi_{NO_2^-}$ at pH 8 (see Figure 5).

The current U.S. EPA drinking water standard for nitrite is 1 ppm as N (71 μm); therefore, the dose dependence of the NO_2^- concentration is of particular interest. In only one case (5 ppm DOC, pH 8, ~300 mJ/cm^2) does the NO_2^- concentration exceed 10% of the standard; however, this is above the German standard of 0.1 ppm as N. If U.S. regulations remain consistent, these data allow an estimate that total UV doses (200−300 nm) of approximately 300−400 mJ/cm^2 can be applied to waters with relatively high DOC and NO_3^- levels while keeping NO_2^- levels below 20% of the drinking water standard. This conclusion is in general agreement with that reached by Peldszus et al. in a study of MPUV at a pilot plant for drinking water treatment (*6*). Although we have presented the total dose in the 200−300-nm range, the germicidal dose needs to be considered for disinfection purposes. Approximating this as 60% of the output from a MP lamp in the 200−300-nm range leads to an estimate of about 160−240 mJ/cm^2 as a conservative upper limit for disinfecting waters high in NO_3^- with MPUV. At the more frequently encountered NO_3^- levels of 0.1−1 ppm as N, this dose could be substantially increased without concern for excessive NO_2^- production. Thus, under the present U.S. regulatory framework and potential future limits in line with the German standards, there should be no need to take special precautions with MP lamps to filter out wavelengths <240 nm during UV disinfection of water at germicidal UV doses below approximately 200 mJ/cm^2.

In evaluating the above results, some additional points should be kept in mind. For example, the complex nature of the NO_3^- photolysis mechanism makes the NO_2^- yield dependent on many parameters, which may be quite variable in real water treatment scenarios. It is probably best, therefore, to conduct tests on a wide range of waters before the conclusions reached above can be generalized. In practice, case-by-case determinations of NO_2^- production rates may be necessary. In addition, NO_3^- photolysis in the presence of aromatic compounds produces nitroaromatics, which pose a health hazard (*32*). The potential for such reactions in individual UV treatment schemes needs to be seriously considered apart from any concerns surrounding NO_2^- formation. Furthermore, it is currently unknown what effects DIC and NOM may have on these photoinduced nitration reactions.

In conclusion, this research demonstrates important roles for NOM and DIC in NO_2^- formation during NO_3^- photolysis, and it extends and complements the work of other researchers to show that NO_2^- formation is unlikely to pose a health concern during MPUV disinfection (*6*). While the effect of DIC seems clearly related to the reaction of CO_2(aq) with $ONOO^-$, the increasing rate of NO_2^- formation with NOM is currently unexplained. Further work to elucidate the reactions responsible for the present results is necessary to clarify the mechanism of NO_2^- formation in natural waters and to allow more accurate assessments of how water quality will impact NO_2^- formation during MPUV disinfection.

Acknowledgments

The authors gratefully acknowledge Travis L. Bastow for assistance with some of the experimental work. Mr. Bastow was supported as a summer intern via a National Science Foundation Research Experience for Undergraduates grant.

Literature Cited

(1) Shin, G.-A.; Linden, K. G.; Faubert, G.; Sobsey, M. D. *Proceedings American Water Works Association Water Quality and Technology Conference*; Salt Lake City, UT, November 5−9, 2000.
(2) Clancy, J. L.; Bukhari, Z.; Hargy, T. M.; Bolton, J. R.; Dussert, B.; Marshall, M. M. *J. Am. Water Works Assoc.* **2000**, *92* (9), 97−104.
(3) von Sonntag, C.; Schuchmann, H.-P. *Aqua* **1992**, *41* (2), 67−74.
(4) Mack, J.; Bolton, J. R. *J. Photochem. Photobiol. A* **1999**, *128*, 1−13.
(5) German Association on Gas and Water. *Technical Standard DVGW 294, UV Systems for Disinfection in Drinking Water Supplies−Requirements and Testing*; 1997.
(6) Peldszus, S.; Andrews, S. A.; Souza, R.; Bolton, J. R.; Dussert, B. W.; Smith, F. *Proceedings American Water Works Association Water Quality and Technology Conference*; Salt Lake City, UT, November 5−9, 2000.
(7) Mark, G.; Korth, H.-G.; Schuchmann, H.-P.; von Sonntag, C. J. *Photochem. Photobiol. A,* **1996**, *101*, 89−103.
(8) Schwarzenbach, R. P.; Gschwend, P. M.; Imboden, D. M. *Environmental Organic Chemistry*; Wiley-Interscience: New York, 1993; Chapter 13.
(9) Hoigné, J.; Faust, B. C.; Haag, W. R.; Scully, F. E. Jr.; Zepp, R. G. In *Aquatic Humic Substances: Influence on Fate and Treatment of Pollutants*; Suffet I. H., MacCarthy P., Eds.; Advances In Chemistry Series 219; American Chemical Society: Washington, DC, 1989; pp 333−362.
(10) Lymar, S. V.; Hurst, J. K. *J. Am. Chem. Soc.* **1995**, *117*, 8867−8868.
(11) Lymar, S. V.; Hurst, J. K. *Chem. Res. Toxicol.* **1996**, *9*, 845−850.
(12) Løgager, T.; Sehested, K. *J. Phys. Chem.* **1993**, *97*, 6664−6669.
(13) Plumb, R. C.; Edwards, J. O.; Herman, M. *Analyst* **1992**, *117*, 1639−1641.
(14) Plumb, R. C.; Edwards, J. O. *J. Phys. Chem.* **1992**, *96*, 3245−3247.
(15) Zafiriou, O. C.; Joussot-Dubien, J.; Zepp, R. G.; Zika, R. G. *Environ. Sci. Technol.* **1984**, *18*, 358A−371A.
(16) Standard Methods. *Standard Methods for the Examination of Water and Wastewater*, 20th ed.; Clesceri, L. S., Greenberg, A. E., Eaton, A. D., Eds.; American Public Health Association: Washington, DC, 1998.
(17) Murov, S. L.; Hug, G. L.; Carmichael, I. *Handbook of Photochemistry*; Marcel Dekker: New York, 1993.
(18) Daniels, M.; Meyers, R. V.; Belardo, E. V. *J. Phys. Chem.* **1968**, *72*, 389−399.
(19) Shuali, U.; Ottolenghi, M.; Rabani, J.; Yelin, Z. *J. Phys. Chem.* **1969**, *73*, 3445−3451.
(20) Warneck, P.; Wurzinger, C. *J. Phys. Chem.* **1988**, *92*, 6278−6283.
(21) Bayliss, N. S.; Bucat, R. B. *Aust. J. Chem.* **1975**, *28*, 1865−1878.
(22) Goldstein, S.; Czapski, G. *Inorg. Chem.* **1997**, *36*, 5113−5117.
(23) Gerasimov, O. V.; Lymar, S. V. *Inorg. Chem.* **1999**, *38*, 4317−4321.
(24) Goldstein, S.; Meyerstein, D.; van Eldik, R.; Czapski, G. *J. Phys. Chem.* **1999**, *103*, 6587−6590.
(25) Coddington, J. W.; Hurst, J. K.; Lymar, S. V. *J. Am. Chem. Soc.* **1999**, *121*, 2438−2443.
(26) Pfeiffer, S.; Gorren, A. C. F.; Schmidt, K.; Werner, E. R.; Hansert, B.; Bohle, D. S.; Mayer, B. *J. Biol. Chem.* **1997**, *272*, 3465−3470.
(27) Uppu, R. M.; Squadrito, G. L.; Pryor, W. A. *Arch. Biochem. Biophys.* **1996**, *327*, 335−343.
(28) Lymar, S. V.; Hurst, J. K. *Inorg. Chem.* **1998**, *37*, 294−301.
(29) Goldstein, S.; Czapski, G. *J. Am. Chem. Soc.* **1998**, *120*, 3458−3463.
(30) Merenyi, G.; Lind, J.; Goldstein, S.; Czapski, G. *Chem. Res. Toxicol.* **1998**, *11*, 712−713.
(31) Denicola, A.; Freeman, B. A.; Trujillo, M.; Radi, R. *Arch. Biochem. Biophys.* **1996**, *333*, 49−58.
(32) Dzengel, J.; Theurich, J.; Bahnemann, D. *Environ. Sci. Technol.* **1999**, *33*, 294−300.

Received for review December 28, 2000. Revised manuscript received April 20, 2001. Accepted April 27, 2001.

ES002043L